Mechanical Properties and Interlaminar Toughness of Cross-Plied Laminates Containing Adhesive Strips

T. L. Norman* and C. T. Sun†
Purdue University, West Lafayette, Indiana 47907

The critical strain energy release rate G_c of graphite/epoxy composites with adhesive strips at the interface is determined using the double cantilever beam test, and comparison is made with composites without adhesive. It is found that delamination fracture toughness increases substantially when adhesive strips are added at the interface, reaching a limiting value for increased adhesive widths. A micromechanical model is developed for stiffness predictions of composites with adhesive strips. A comparison with experimental values is found in good agreement and indicates a reduction in stiffness approximately equal to the percentage of adhesive used in the composite. Strength tests are performed and showed similar reductions for unnotched specimens with adhesive strips. Strength reductions for notched specimens with adhesive are found to vary, depending on notch size and adhesive width.

Introduction

DELAMINATION is a failure mode commonly found in graphite/epoxy laminated composite materials subjected to impact loading.[1,2] This failure mode occurs at the lamina interface and can propagate, affecting the structural integrity, especially the compressive strength. Although delamination can lead to widespread damage within the structure, it is a failure mode that absorbs impact energy. If delamination is completely suppressed, impact energy could result in fiber breakage, which would have a greater effect on laminate strength.

One method being considered for interface toughening is the use of adhesive layers. By placing tough adhesive films along the interfaces of the laminas, Chan et al.[3] demonstrated that edge delamination in coupon laminated specimens subjected to in-plane tension could be suppressed. Sun and Rechak[4] employed a similar method to delay the initiation of and reduce the extent of delamination induced by impact loading. In their paper, the mechanisms provided by the presence of interlaminar adhesive layers in reducing impact damage was studied. It was found that adhesive layers included in a composite laminate could increase the contact area and, as a result, reduce the transverse shear concentration effect. This, together with the toughened interfacial property, resulted in less delamination. In a follow-up paper, Rechak and Sun[5] developed a guide for optimal use of adhesive layers to minimize the use of adhesives.

The interfacial toughness of graphite/epoxy systems with adhesive at the midplane of unidirectional laminates has been investigated.[6-8] Results from these studies clearly indicate that the use of adhesive in the plane of crack propagation can increase the Mode I and Mode II critical strain energy release rates substantially. Although adhesive layers increase the interfacial toughness, they also add weight and reduce stiffness and compressive strength. Moreover, the suppression of delamination may result in massive fiber breakage when impact velocity exceeds a certain threshold velocity.[4]

In a paper by Sun and Norman,[9] delamination and bending residual strength tests of graphite/epoxy laminated composites with adhesive strips subjected to transverse impact loading was investigated. This study concluded that delamination can be confined in a region within the adhesive strips in laminated composites subjected to impact loading. It was shown that adhesive strips resulted in some loss in strength of the composite before impact. However, bending residual strength at higher velocities in the specimens with adhesive is slightly higher than in the specimens without adhesive. The effect of adhesive strips on the retention of residual compressive strength after impact is expected to be even more significant since compressive strength is very sensitive to the size of delamination. Delamination due to low velocity impact of composites with adhesive has also been investigated by other authors where similar results were found.[6]

The purpose of this research is to develop a concept of laminate design that will allow delamination to occur in the region of impact but will keep it from propagating excessively. This concept, referred to as the controlled-damage concept, uses adhesive strips in laminated composites. In this paper, the fracture toughness of graphite/epoxy laminated composite with adhesive strips at the interface is determined in order to develop an analytical model later to predict the capability of delamination arrest provided by the adhesive strips in laminated composites. In addition, stiffness and notched and unnotched strength for laminated composites with the controlled-damage concept were investigated.

Strength and Stiffness

The stiffness and notched and unnotched strength of graphite/epoxy composite specimens toughened with adhesive strips (controlled-damage specimens) are investigated experimentally, and a comparison is made with specimens without adhesive strips (plain specimens). The laminate material constants for controlled-damage composites are determined from a micromechanical model and laminated plate theory.

Laminate Design

Figure 1 shows the controlled-damage design concept for the graphite/epoxy laminate with adhesive strips for a [0/90/0] laminate. As seen in the figure, the outer ply of each lamina contains the American Cyanamid Company FM-1000 adhesive and Hercules AS4/3501-6 graphite/epoxy prepreg tape

Presented as Paper 89-1349 at the AIAA/ASME/ASCE/AHS/ASC 30th Structures, Structural Dynamics, and Materials (SDM) Conference, Mobile, AL, April 3-5, 1989; received Aug. 2, 1989; revision received March 26, 1990.

*Currently Assistant Professor, Department of Mechanical and Aerospace Engineering, West Virginia University.

†Professor, School of Aeronautics & Astronautics. Associate Fellow AIAA.

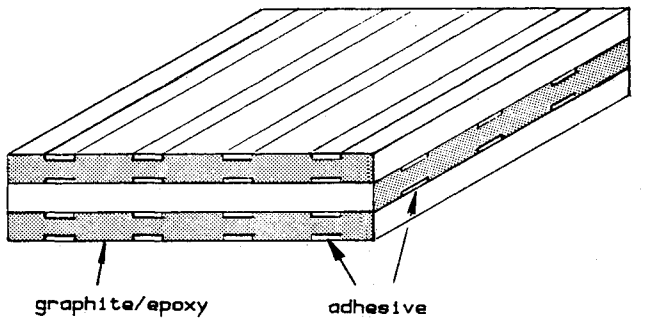

Fig. 1 Controlled damage concept for [0/90/0] laminate.

cut into strips. Between the outer plies only graphite/epoxy composite is found. The ply containing the adhesive is formed by alternating graphite/epoxy with adhesive strips, the width of the strips depending on the particular design chosen. When 0- and 90-deg laminae are placed together, the adhesive strips form a square mesh arrangement at the interface.

Two different controlled-damage laminate designs were used, one containing 25.4 mm (1.0 in.) width graphite/epoxy alternating with 12.7 mm (0.5 in.) width adhesive strips, and the other containing 12.7 mm width graphite/epoxy alternating with 6.35 mm (0.25 in.) width adhesive strips on the outermost layers. Both designs have a layup geometry of $[0_a/0/0_a/90_a/90/90_a/0_a/0/0_a/90_a/90/90_a/0_a/0/0_a]$ where subscript "a" denotes adhesive strips present in the designated ply. Plain specimens were cut from fabricated graphite/epoxy panels with layup geometry of $[0_3/90_3/0_3/90_3/0_3]$ for comparison with the controlled-damage specimens.

Experimental Procedure

Controlled-damage composite laminates with 6.35 mm and 12.7 mm width adhesive strips were cut into transverse and longitudinal specimens of widths approximately equal to 38.1 mm (1.5 in.) and 76.2 mm (3.0 in.) respectively. Specimens of approximately the same widths were cut from plain laminates. End tabs were fabricated from fiberglass and attached to the specimen ends with an adhesive. The gauge length of the specimens was 15.24 cm (6.0 in.). Strain gages were attached to a number of plain and controlled-damage specimens in the longitudinal and transverse direction on both the graphite/epoxy and the adhesive surfaces.

Notched specimens were obtained by drilling 6.35-mm diam holes in plain and controlled-damage specimens in various locations to obtain a number of different notched configurations. The layup geometry in the region of the notch is identical to that previously described. Two notched geometries for controlled-damage specimens using 12.7 mm and 6.35 mm width adhesive are shown in Fig. 2.

Specimens were tested under load control on a closed-loop MTS test machine. Load-strain curves were obtained by plotting on the Omnigraph 2000 recorder via a Wheatstone bridge circuit and the Tektronix TM 502 Differential Amplifier. A number of specimens were tested until failure for ultimate load.

Theoretical Model

Theoretical predictions of stiffness for controlled-damage composites are made using a micromechanical model. A building lamina with a layup geometry of $[0_a/0/0_a]$ is used to develop the model. Figure 3 shows the three-ply building lamina consisting of graphite/epoxy and hybrid regions. As seen in the figure, the hybrid region contains both graphite/epoxy composite and adhesive strips. Laminate material constants are determined by first using lamination theory to determine the effective material constants for the hybrid region: E_1^h, E_2^h, G_{12}^h, ν_{12}^h. Then the micromechanical model is used to

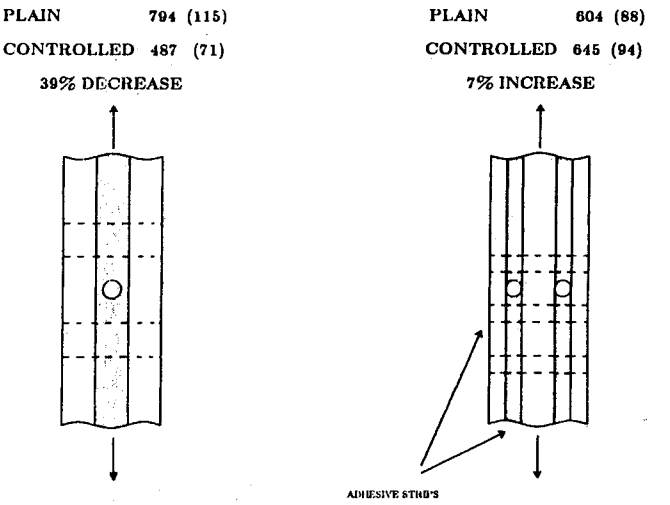

Fig. 2 Notched configurations and strengths of plain and controlled-damage specimens.

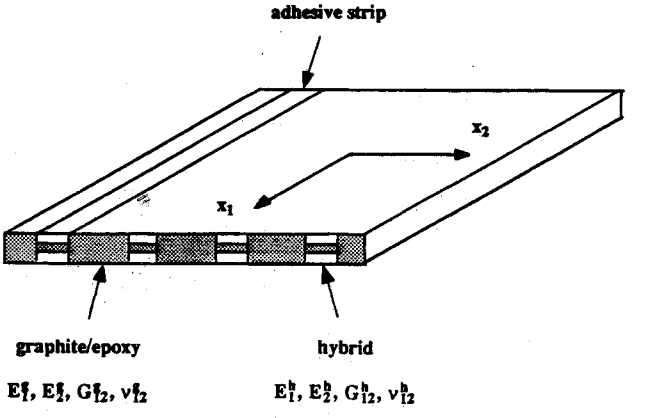

Fig. 3 Idealized two-dimensional fiber-reinforced composite lamina with adhesive strips.

determine the effective moduli for the building lamina. The building lamina moduli are then used in lamination theory to determine the laminate material constants. The micromechanical model is developed as follows.

Consider an idealized two-dimensional fiber-reinforced composite consisting of graphite/epoxy and hybrid regions as shown in Fig. 3. Plane stress parallel to x_1-x_2 plane is assumed. The graphite/epoxy and hybrid regions have elastic constants E_1^g, E_2^g, G_{12}^g, ν_{12}^g and E_1^h, E_2^h, G_{12}^h, ν_{12}^h, respectively. For the foregoing representations of the material constants, the g and h refer to the graphite/epoxy and hybrid constituents, respectively.

The composite is modeled as a two-dimensional orthotropic solid whose stress-strain relations are given by

$$\begin{Bmatrix} \bar{\sigma}_{11} \\ \bar{\sigma}_{22} \\ \bar{\sigma}_{12} \end{Bmatrix} = \begin{bmatrix} Q_{11} & Q_{12} & 0 \\ Q_{12} & Q_{22} & 0 \\ 0 & 0 & Q_{66} \end{bmatrix} \begin{Bmatrix} \bar{\epsilon}_{11} \\ \bar{\epsilon}_{22} \\ \bar{\gamma}_{12} \end{Bmatrix} \tag{1}$$

or

$$\begin{Bmatrix} \bar{\epsilon}_{11} \\ \bar{\epsilon}_{22} \\ \bar{\gamma}_{12} \end{Bmatrix} = \begin{bmatrix} \frac{1}{E_1} & -\frac{\nu_{12}}{E_1} & 0 \\ -\frac{\nu_{12}}{E_1} & \frac{1}{E_2} & 0 \\ 0 & 0 & \frac{1}{G_{12}} \end{bmatrix} \begin{Bmatrix} \bar{\sigma}_{11} \\ \bar{\sigma}_{22} \\ \bar{\sigma}_{12} \end{Bmatrix} \tag{2}$$

where the elements Q_{ij} are the effective reduced stiffnesses, and $\bar{\sigma}_{ij}$ and $\bar{\epsilon}_{ij}$ are the average stress and strain for a macroscopically homogeneous stress or deformation field on a respective volume element.

For the graphite/epoxy and hybrid regions, the average stress and strain can be written as

$$\bar{\sigma}_{ij} = \frac{1}{V}\left(\int_{V_g} \sigma_{ij}^{g}(x,y,z)\,dV + \int_{V_h} \sigma_{ij}^{h}(x,y,z)\,dV\right) \tag{3}$$

$$\bar{\epsilon}_{ij} = \frac{1}{V}\left(\int_{V_g} \epsilon_{ij}^{g}(x,y,z)\,dV + \int_{V_h} \epsilon_{ij}^{h}(x,y,z)\,dV\right) \tag{4}$$

respectively. In Eqs. (3) and (4), V_g denotes the volume of the graphite/epoxy region, V_h denotes the hybrid region, σ_i^g (ϵ_i^g) is the stress (strain) field in the graphite/epoxy, and average σ_i^h (ϵ_i^h) is the stress (strain) field in the hybrid region. The stress/strain relations for the graphite/epoxy composite and the hybrid constituents are, respectively,

$$\begin{Bmatrix} \epsilon_{11}^{g} \\ \epsilon_{22}^{g} \\ \gamma_{12}^{g} \end{Bmatrix} = \begin{bmatrix} \frac{1}{E_1^g} & -\frac{\nu_{12}^g}{E_1^g} & 0 \\ -\frac{\nu_{12}^g}{E_1^g} & \frac{1}{E_2^g} & 0 \\ 0 & 0 & \frac{1}{G_{12}^g} \end{bmatrix} \begin{Bmatrix} \sigma_{11}^{g} \\ \sigma_{22}^{g} \\ \sigma_{12}^{g} \end{Bmatrix} \tag{5}$$

$$\begin{Bmatrix} \epsilon_{11}^{h} \\ \epsilon_{22}^{h} \\ \gamma_{12}^{h} \end{Bmatrix} = \begin{bmatrix} \frac{1}{E_1^h} & -\frac{\nu_{12}^h}{E_1^h} & 0 \\ -\frac{\nu_{12}^h}{E_1^h} & \frac{1}{E_2^h} & 0 \\ 0 & 0 & \frac{1}{G_{12}^h} \end{bmatrix} \begin{Bmatrix} \sigma_{11}^{h} \\ \sigma_{22}^{h} \\ \sigma_{12}^{h} \end{Bmatrix} \tag{5}$$

For a representative element, we assume for any general deformation

$$\epsilon_{11}^g = \epsilon_{11}^h = \bar{\epsilon}_{11}\text{: constant strain} \tag{7a}$$

$$\sigma_{22}^g = \sigma_{22}^h = \bar{\sigma}_{22}\text{: constant stress} \tag{7b}$$

$$\sigma_{12}^g = \sigma_{12}^h = \bar{\sigma}_{12}\text{: constant stress} \tag{7c}$$

where Eq. (7a) ensures nonseparation between graphite/epoxy and hybrid regions, while Eqs. (7b) and (7c) satisfy the continuity of stresses at their interface.

Since the stresses and strains are constant in both constituents, we have from Eqs. (3) and (4)

$$\bar{\sigma}_{11} = \nu_g \sigma_{11}^g + \nu_h \sigma_{11}^h \tag{8a}$$

$$\bar{\epsilon}_{22} = \nu_g \epsilon_{22}^g + \nu_h \epsilon_{22}^h \tag{8b}$$

$$\bar{\gamma}_{12} = \nu_g \gamma_{12}^g + \nu_h \gamma_{12}^h \tag{8c}$$

where ν_g and ν_h are the volume fractions of the graphite/epoxy and hybrid regions, respectively.

By considering a state of simple tension in the x_1 direction, the effective longitudinal modulus E_1 can be determined from Eq. (8a) and the constant strain assumption of Eq. (7a). The effective Poisson ratio ν_{12} is found from the preceding assumption and Eq. (8b). Applying simple shear, the in-plane effective shear modulus is determined from Eq. (8c) and the constant stress assumption of Eq. (7c). The effective transverse modulus E_2 is obtained by applying simple tension in the x_2 direction. Then Eq. (8b) is used along with the constant stress assumption of Eq. (7b).

After some manipulations of the above equations, effective material properties (micromechanical model equations) are found to be

$$E_1 = \nu_g E_1^g + \nu_h E_1^h \tag{9}$$

$$\nu_{12} = \nu_g \nu_{12}^g + \nu_h \nu_{12}^h \tag{10}$$

$$\frac{1}{G_{12}} = \frac{\nu_g}{G_{12}^g} + \frac{\nu_h}{G_{12}^h} \tag{11}$$

$$\frac{1}{E_2} = \left(\frac{\nu_g}{E_2^g} + \frac{\nu_h}{E_2^h}\right) - \frac{\nu_g \nu_h (\nu_{12}^g E_1^h - \nu_{12}^h E_1^g)^2}{E_1^h E_1^g (\nu_g E_1^g + \nu_h E_1^h)} \tag{12}$$

For a three-ply building lamina, ν_h is 1/3 and ν_g is 2/3, representing the volume fraction of the graphite/epoxy and hybrid regions, respectively, for both the 6.35-mm and 12.7-mm width adhesive. Using the properties for AS4/3501-6 graphite/epoxy

$$E_1^g = 138 \text{ GPa (20.0 Msi)}$$

$$E_2^g = 9.99 \text{ GPa (1.45 Msi)}$$

$$G_{12}^g = 5.52 \text{ GPa (0.8 Msi)}$$

$$\nu_{12}^g = 0.3 \tag{13}$$

and the properties of FM-1000 adhesive

$$E_1^a = 1.72 \text{ GPa (0.25 Msi)}$$

$$E_2^a = 1.72 \text{ GPa (0.25 Msi)}$$

$$G_{12}^a = 0.648 \text{ GPa (0.094 Msi)}$$

$$\nu_{12}^a = 0.33 \tag{14}$$

The effective material constants for the hybrid region as determined from laminated plate theory are

$$E_1^h = 47.1 \text{ GPa (6.83 Msi)}$$

$$E_2^h = 4.60 \text{ GPa (0.67 Msi)}$$

$$G_{12}^h = 2.27 \text{ GPa (0.33 Msi)}$$

$$\nu_{12}^h = 0.31 \tag{15}$$

The micromechanical model equations, [Eqs. (9–12)] and Eqs. (13) and (15) are used to determine the effective moduli for the building lamina,

$$E_1 = 108 \text{ GPa (15.61 Msi)}$$

$$E_2 = 7.20 \text{ GPa (1.04 Msi)}$$

$$G_{12} = 3.74 \text{ GPa (0.54 Msi)}$$

$$\nu_{12} = 0.30 \tag{16}$$

The building lamina moduli are now used in the formulation of $[Q]$ in Eq. (1). The laminated plate theory is then employed to predict the overall laminated properties.

Results

Load-strain curves from material testing are used to obtain the experimental material properties. The strains in the composite and adhesive regions are about the same. The average strain is calculated according to Eq. (4).

Table 1 Laminate properties for plain and controlled-damage composites with layup geometry of $[0_3/90_3/0_3/90_3/0_3]$

	Specimen Type	E_x GPa (Msi)	E_y Gpa (Msi)	ν_{xy}
Experimental	plain	85.3 (12.4)	59.0 (8.6)	0.045
	controlled	66.3 (9.6)	49.4 (7.2)	0.051
Predicted	plain	87.1 (12.6)	61.4 (8.9)	0.049
	controlled	67.8 (9.8)	47.6 (6.9)	0.046

Table 2 Laminate tensile strength for unnotched plain and controlled-damage composite specimens with layup geometry of $[0_3/90_3/0_3/90_3/0_3]$

Specimen type	Plain	Controlled	Controlled
Adhesive width, mm (in.)	——	6.35 (0.25)	12.7 (0.5)
Laminate strength MPa (ksi)	1018 (148)	803 (116)	790 (114)

Table 1 shows the experimental and predicted laminate properties for the plain and controlled-damage specimens normalized to a nominal ply thickness of 0.132 mm (0.0052 in.). Experimental results represent an average of 38.1 mm and 76.2 mm width specimens when both were tested. As seen in the table, the longitudinal and transverse stiffness of the controlled-damage specimen is reduced as compared to the plain specimen. The reduction in stiffness is determined to be approximately equal to the percentage of adhesive used in the controlled-damage specimen, which is approximately equal to 22% in both the longitudinal and transverse fiber directions. Experimental material constants are found in good agreement with those predicted using effective material properties for the controlled damage specimens. Table 2 shows the tensile strength results for the plain and the controlled specimens. Results shown have been normalized to a ply thickness of 0.132 mm. Results indicate a 20 and 24% reduction in longitudinal strength for the controlled specimens with 6.35 mm and 12.7 mm width adhesive, respectively. As in the case of stiffness, this is approximately equal to the percentage of adhesive used in the longitudinal and transverse fiber direction.

Strength results for two notched configurations tested are shown in Fig. 2. The two cases shown represent the largest increase and decrease in strength for all configurations considered. Note that the strengths are based on gross section and are an average of three specimens for each geometry. Notched configurations using 12.7 mm width adhesive with a 6.35 mm hole show a substantial strength reduction ranging from 19 to 39% Those using 6.35 mm width adhesive show more favorable results, with strength ranging from a 3% decrease to a 7% increase. Thus, although the use of adhesive in composites reduces the strength in unnotched specimens, certain configurations can give rise to an increase in notched strength.

Delamination Fracture Toughness

The double cantilever beam (DCB) test has been used by many researchers for determining mode I interlaminar fracture toughness of both unidirectional and multidirectional fiber reinforced composites.[6-8, 10-14] In this study, the DCB test is used to determine the critical strain energy release rate (G_c) at a 0/90 interface of graphite/epoxy composites with adhesive strips, and a comparison is made with plain specimens. The adhesive width is varied to determine a limiting value of G_c.

Experimental Procedure

Hercules AS4/3501-6 graphite/epoxy prepreg tape was fabricated into panels with layup geometry of $[(0/90)_9/0]$. The layup was chosen to avoid bending cracks on the outer plies during loading. During fabrication, a thin teflon film was inserted at the midplane of the composite laminate between the 0 and 90 deg laminas to establish a precrack. Composite panels were also fabricated with American Cyanamid Company; FM-1000 adhesive cut into strips of widths 6.35, 12.7, 25.4 mm, and 38.1 mm inserted at the midplane of the laminate adjacent to the 90-deg ply. A total of three adhesive strips were used at the midplane of each DCB specimen.

Specimens 2.54 cm wide and 22.86 cm (9.0 in.) long were cut from the composite panels. Figure 4 shows a representative composite DCB specimen with adhesive. Initial crack size for plain specimens established by the teflon precrack during fabrication was 38.1 mm. In the specimens with adhesive, strips were located at distances of 38.1 mm (1.5 in.), 63.5 mm (2.5 in.), and 88.9 mm (3.5 in.), and cracks propagated from the teflon precrack to the adhesive. Then the precrack to adhesive is considered the total distance to the adhesive, as above. Metal hinges were attached to the ends of the specimens to allow unrestrained rotation during loading. The free ends of hinges were placed in the loading machine grips.

Figure 5 shows the DCB testing configuration used on a Capitol electromechanical servo-driven testing machine at a crosshead rate of 0.042 mm/s (0.1 in./min). Because the composite specimens are very compliant[6,7] and displacements are relatively large, crack opening displacements were equated to head travel and were plotted against load on an x-y plotter. Crack extensions were monitored visually.

Data Analysis

Three methods of analyzing the DCB have frequently been used to determine the delamination fracture toughness G_c[10]: area method, beam analysis method, and a generalized empirical method. The beam analysis method was used in this study.

In the beam analysis method, the strain energy release rate is given by[14]

$$G = \frac{P^2 a^2}{bEI} \tag{17}$$

where P is the applied load a is the crack length, b is the specimen width, and EI is the beam bending stiffness. For a composite laminate under cylindrical bending, the bending stiffness can be written in terms of D_{11} from the classical lamination theory. Thus, we obtain the critical strain energy

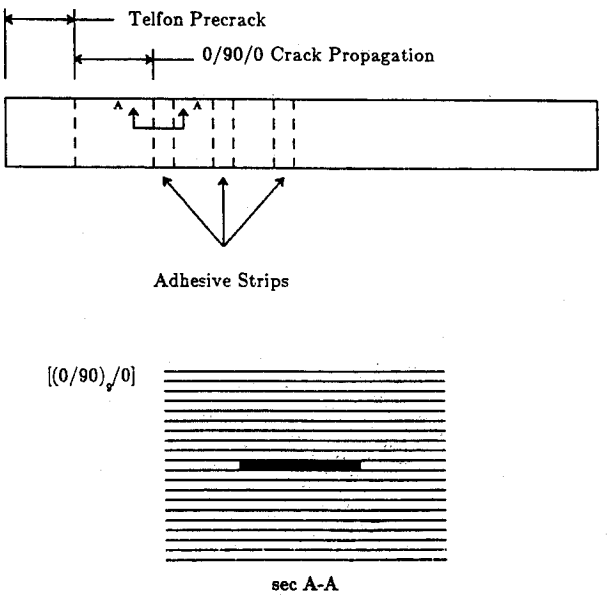

Fig. 4 Composite DCB specimen with adhesive strips.

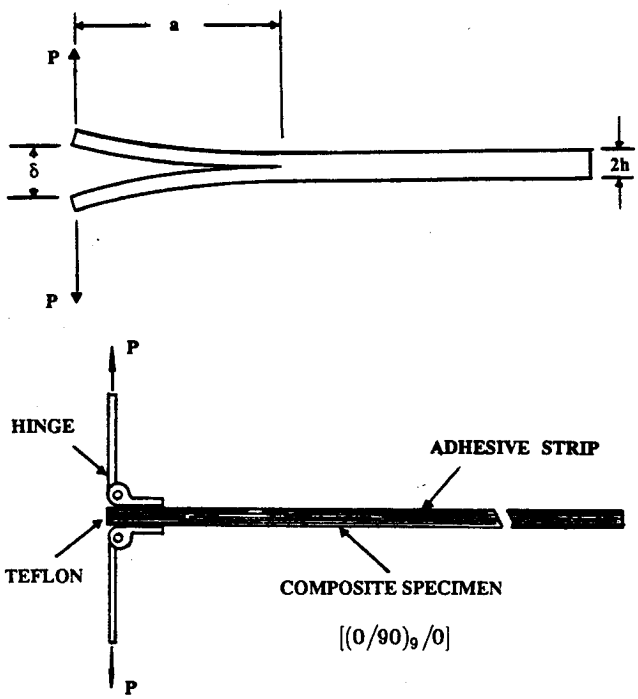

Fig. 5 Double cantilever beam specimen geometry for measurement of delamination fracture toughness.

release rate for the DCB per unit width b

$$G_c = \frac{P_c^2 a^2}{2b}\left[\frac{1}{D_{11}^{(1)}} + \frac{1}{D_{11}^{(2)}}\right] \tag{18}$$

where P_c is the critical value of P associated with the onset of crack growth. Note that D_{11} is different for the upper and lower beams since they are unsymmetric about the crack plane. Assuming that $D_{11}^{(1)}$ corresponds to the layup geometry of $[(0/90)_4/0]$ and that $D_{11}^{(2)}$ corresponds to the layup geometry of $[0/90]_5$, we find that

$$D_{11}^{(1)} = 0.34\ N - m^2\ (118\ \text{lb} - \text{in.}^2)$$

$$D_{11}^{(2)} = 0.36\ N - m^2\ (126\ \text{lb} - \text{in.}^2) \tag{19}$$

based on material properties of AS4/3501-6 given by Eq. (13).

Results

Crack propagation at the 0/90 interface of the DCB specimen is between the upper and lower 0 = deg plies of the interface through the 90-deg ply (crack branching). A typical crack plane shows the coarse appearance of the crack surface in the region of crack branching between the end of the teflon precrack and the beginning of the adhesive strip. When the crack reaches the adhesive at the interface, after a substantial increase in loading, some of the fibers of the upper or lower 0-deg ply break (fiber bridging). The crack then propagates past the adhesive into the upper or lower 0-deg plies. Here, there are small amounts of adhesive present, depending upon the amount that migrates into the lamina during curing. Note that after the crack propagates past the first adhesive strip, it is no longer at the same interface of the remaining two strips. This type of failure occurs for specimens with adhesive widths of 12.7 and 25.4 mm. For specimens with adhesive widths larger than 25.4 mm, delamination frequently occurred at a lower critical load at an interface other than the one containing adhesive. This fracture data were not used.

Critical load is plotted against crack length in Fig. 6 for plain specimens and specimens with adhesive. The critical load is defined here as the load at which delamination crack propagation occurs. As seen in the figure, critical loads for specimens with adhesive are substantially higher than for the plain specimens. It is observed that the critical loads for the specimens with 6.35 and 12.7 mm width adhesive are relatively close in value.

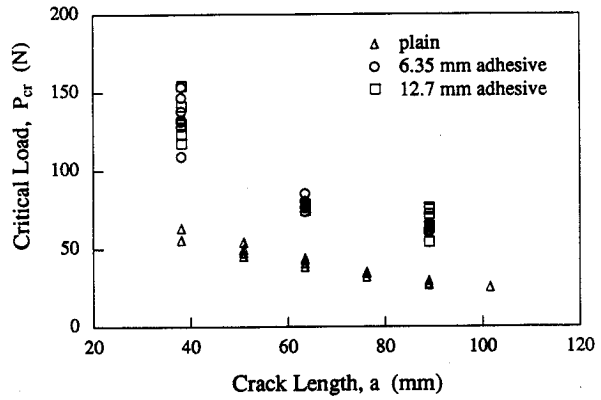

Fig. 6 Critical load plotted against crack length for DCB plain specimens and specimens with adhesive strips.

Table 3 Variation of DCB critical strain energy release rate (G_c) with crack length as determined by beam analysis method

Specimen type		Plain	Controlled	Controlled
Adhesive width, mm (in.)		——	6.35 (0.25)	12.7 (0.50)
Crack length	38.1 (1.5)	——	2280 (13.0)	2270 (12.9)
a mm (in.)	50.8 (20)	497 (2.8)	——	——
	63.5 (2.5)	555 (3.2)	2140 (12.2)	2100 (12.0)
	76.2 (3.0)	523 (3.0)	——	——
	89.9 (3.5)	471 (2.7)	2700 (15.4)	3100 (17.7)
	101.6 (4.0)	510 (2.9)	——	——
Average G_c NM (lb/in.)		511 (2.9)	2340 (13.5)	2490 (14.2)

Table 3 shows critical strain energy release rates for DCB plain specimens and specimens with adhesive as determined by the beam analysis method. As seen in Table 3, values of G_c for the 0/90 interface are substantially higher than G_{Ic} for unidirectional laminates.[13] It has been observed that use of the DCB test for multidirectional laminates often results in high values of G_{Ic} as compared to unidirectional composites.[12] This could be due to crack branching similar to that observed in this study. Since the delamination crack propagation at the 0/90 interface described previously is not in the classical Mode I sense, total G_c is calculated instead of G_{Ic}, and G_c is an indication of the energy required for delamination crack propagation.

Average values of G_c are given in Table 3 for crack lengths shown representing four plain, sixteen 6.35 mm width adhesive and fifteen 12.7 mm with adhesive specimens. It is observed from the table that the delamination fracture toughness increases substantially when adhesive is added. The G_c for the plain specimens remains nearly constant for different crack dimensions a approximately equal to 525 N/m (3.0 lb/in.). For the specimens with adhesive, G_c remains nearly constant for crack dimensions 38.1 and 63.5 mm, whereas for crack dimension 88.9 mm, there is an increase. Neglecting G_c for this crack dimension (since in practicality the grid using the controlled-damage concept will usually be less than 88.9 mm), average G_c is approximately equal to 2190 N/m (12.5 lb/in.). Thus, the delamination fracture toughness between a 0/90 interface increases approximately four times when adhesive strips are added. For specimens with adhesive widths larger than 12.7 mm, G_c was determined to be slightly less than the values tabulated in Table 3. This indicates that increasing the adhesive width beyond a certain point may not result in a higher fracture toughness.

Conclusions

The effective moduli for a lamina with adhesive have been determined from a micromechanical model and used with lamination theory to predict the material constants for controlled-damage composites. Experimental material constants are found in good agreement with those predicted. Strength and stiffness results indicate reductions for unnotched controlled-damage specimens approximately equal to the percentage of adhesive used in the specimen. For notched specimens, strength reductions were found to vary for different notched configurations; however, it was determined that in some cases the notched strength can improve with the use of adhesive.

Fracture toughness at the 0/90 degree interface of a graphite/epoxy laminate with adhesive strips has been determined. Critical load plotted against cracks in specimens showed critical loads substantially higher for the specimens with adhesive inlays than for plain specimens. The G_c was found to increase approximately four times in the specimen with adhesive as compared to the plain specimen. It was determined that fracture toughness increases up to a point and remains nearly constant. Determining fracture toughness allows the author to proceed with the development of an analytical model to predict the delamination arrest capability provided by adhesive strips.

Although using adhesive strips may reduce laminate strength, such reductions can be minimized by increasing the spacing between strips. An even better solution is to place fibers in the adhesive to enhance its stiffness and strength. This new approach is currently under investigation.

Acknowledgment

This work was supported by the Office of Naval Research under Contract N00014-84-K-0554 and McDonnell Aircraft Company. The technical monitors are Y. Rajapakse (ONR), Lee Gause (NADC), and R. S. Behrens (McAir).

References

[1]Takeda, N., Sierakowski, R. L., Malvern, L. E., "Microscopic Observations of Cross Sections of Impacted Composite Laminates," *Composite Technology Review*, Vol. 4, No. 2, 1982, pp. 40–44.

[2]Joshi, S. P., and Sun, C. T., "Impact Induced Fracture in a Laminated Composite," *Journal of Composite Materials*, Vol. 19, No. 2, 1985, pp. 51–66.

[3]Chan, W. S., Rogers, C., and Aker, S., "Improvement of Edge Delamination Strength Using Adhesive Layers," *Composite Materials Testing and Design, 7th Conference, ASTM STP 893*, edited by J. M. Whitney, American Society for Testing and Materials, Philadelphia, PA, 1986, pp. 266–285.

[4]Sun, C. T., and Rechak, S., "Effect of Adhesive Layers on Impact Damage in Composite Laminates," *Composite Material Testing and Design, 8th Conference, ASTM STP 972*, edited by J. D. Whitcomb, American Society for Testing and Materials, Philadelphia, PA, 1988.

[5]Rechak, S., and Sun, C. T., "Optimal Use of Adhesive Layers in Reducing Impact Damage in Composite Laminates," *Composite Structures 4, Proceedings of the 4th International Conference on Composite Structures*, Elsevier, London, July 27-29, 1987, pp. 2.18–2.31.

[6]Eisenmann, J. R., and Ulman, D. A., "Adhesive Strip Concept for Delamination Arrestment," U.S. Air Force, AFWAL-TR-85-3120, 1985.

[7]Mall, S., and Johnson, W. S., "Characterization of Mode I and Mixed Mode Failure of Adhesive Bonds Between Composite Adherends," *Composite Materials: Testing and Design, 7th Conference, ASTM STP 893*, edited by J. M. Whitney, American Society for Testing and Materials, Philadelphia, PA, 1986, pp. 322–334.

[8]Browning, C. E., and Schwartz, H. S., "Delamination Resistant Composite Concepts," *Composite Materials: Testing and Design, 7th Conference, ASTM STP 893*, edited by J. M. Whitney, American Society for Testing and Materials, Philadelphia, PA, 1986, pp. 256–265.

[9]Sun, C.T., and Norman, T. L., "Design of Laminated Composite with Controlled-Damage Concept," *Proceedings of the American Society for Composites, 3rd Technical Conference*, Seattle, Washington, Sept. 26–28, 1988.

[10]Whitney, J. M., Browning, C. E., and Hoogsteden, W., "A Double Cantilever Beam Test for Characterizing Mode I Delamination of Composite Materials," *Journal of Reinforced Plastics and Composites*, Vol. 1, Oct. 1982, pp. 297–313.

[11]Wilkins, D. J., Eisenmann, J. R., Camin, R. A., Margolis, W. S., and Benson, R. A., "Characterizing Delamination Growth in Graphite-Epoxy," *Damage in Composite Materials, ASTM STP 775*, edited by K. L. Reifsnider, American Society for Testing and Materials, Philadelphia, PA, 1982, pp. 168–183.

[12]Nicholls, D. J., and Gallagher, J. P., "Determination of G_{Ic} in Angle Ply Composites Using a Cantilever Beam Test Method," *Journal of Reinforced Plastics and Composites*, Vol. 2, 1983, pp. 2–17.

[13]Aliyu, A. A., and Daniel, I. M., "Effects of Strain Rate on Delamination Fracture Toughness of Graphite/Epoxy," *Delamination and Debonding of Materials, ASTM STP 876*, edited by W. S. Johnson, American Society for Testing and Materials, Philadelphia, PA, 1985, pp. 336–348.

[14]Daniel, I. M., Shareef, I., and Aliyu, A. A., "Rate Effects on Delamination Fracture Toughness of a Toughened Graphite/Epoxy," *Toughened Composites, ASTM STP 937*, edited by N. J. Johnston, American Society for Testing and Materials, Philadelphia, PA, 1987, pp. 260–274.